Real-time Global Earthquake Characterization

U.S.G.S Award No. 05HQGR0173

Final Technical Report

Principal Investigator Dr. Chen Ji
Institute of Crustal Studies, University of California, Santa Barbara, CA, 93106
805.893.2923–phone : 805.893.2314–fax : email- ji@geol.ucsb.edu

Introduction

The great Sumatra-Andaman island earthquake reminds us the natural hazards caused by great Earthquakes in a hard way. When such tragedies occur, quick ground shaking estimates are very useful for local governments to evaluate the damage and to allocate their resources accordingly. The ShakeMap method developed under the *TriNet* project [*Wald et al.*, 1999] provides a tool to obtain such information using observed ground motion time histories combined with estimates from suitable attenuation relationships. However, it requires a dense distribution of real-time reporting strong motion stations, which are only available in a limited number of urban areas such as the Los Angeles basin, San Francisco, Seattle, Salt Lake City, and parts of Japan and Taiwan. In most seismically active regions, there is no such network or the station density is insufficient to provide optimal results. Because such networks are very costly, we expect few improvements in the near future, particularly for the under-developed countries where the earthquake hazard is extreme**.**

The recent development in inverse methodology and deployments of modern broadband instruments make it possible to construct a rough slip history with just a teleseismic dataset. Using the 1999 Chi-Chi and 2002 Denali earthquakes as an example, we have proved that such a model can then be used to predict the ground shaking in the near-fault region, and provide the basis for gauging the overall impact of the earthquake. During the last several years, we have been developing an automatic system and studied over 10 magnitude 7 and larger earthquakes. Some of them have been incorporated into the big earthquake posters made by NEIC. Two recent magnitude 8.5 and larger earthquakes, the 2004 Sumatran-Andaman and 2005 Nias earthquakes have showed the limitation of current methodology. We have developed method to investigate large earthquakes by joint inverting the teleseismic body waves and long period surface waves, under the support of this grant.

Joint inversions of teleseismic body and surface waves

For a shallow focus source, the intervals between P and PP, and S and SS phases in teleseismic distances (for $30^o<\Delta<90^o$) are usually free of significant teleseismic phases. These clear windows have been used to routinely estimate the rupture processes of global large earthquakes [e.g., *Kikuchi and Kanamori*, 1991]. However, for the events with long durations, this dataset could not well constrain the total scalar seismic moment [e.g., *Beck and Ruff*, 1987; *Ekstrom*, 1989; *Kikuchi and Fukao*, 1987]. *Ekstrom* [1989] proposed the

very broadband inversion, which combined the body waves and long period surface waves together, to improve the resolution of both focal mechanism and scalar seismic moment of point sources. For the same reason, we had proposed to develop quick finite fault inverse method based on both teleseismic body waves and long period surface waves. However, our further study indicated that the improvements caused by additional surface waves are not limited to total seismic moment only.

Figure 1 shows a synthetic example using the source-receiver geometry of the 2004 Sumatra-Andaman earthquake. We put the hypocenter at the location of the Harvard CMT of this event and calculate the synthetic seismograms at station GRFO (azimuth=319° and distance=84°). Two sources are used. The first one has a seismic moment of 8x10^{22} Nm and a dip of 6° to the northeast. And the second source has a seismic moment of 4x10^{22} Nm and a dip of 12°. The vertical synthetic seismograms of two sources are virtually identical as expected, suggesting a tradeoff between seismic moment and fault dip based on Rayleigh waves only [e.g., *Kanamori and Given*, 1981]. The amplitude of transverse component, in contrast, is directly proportional to the seismic moment, i.e., carefully analyzing the three component surface waves could resolve this famous trade-off. After we define the rupture area (i.e., using the directivity effect at different stations), any changes in M_o implies changes in fault slip, which usually correlates directly with the amplitude of local strong ground motion. The result is crucial for a quick hazard assessment.

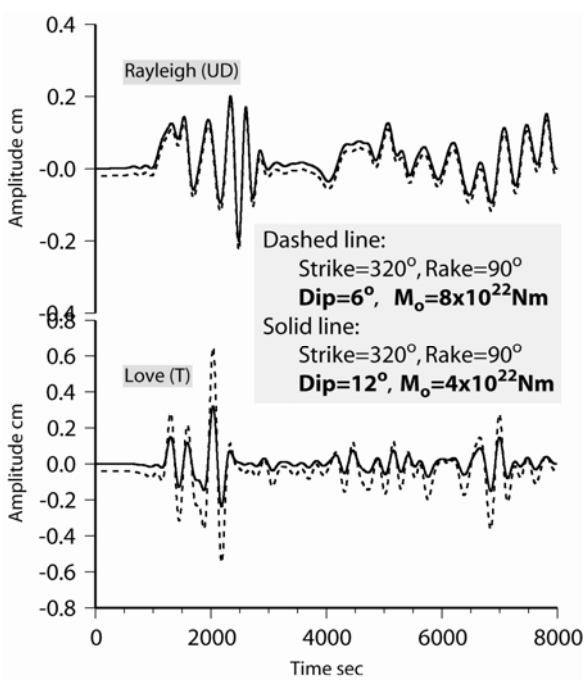

Figure 1. Synthetic seismograms at station GRFO (epicenter distance 84°, azimuth 319°) for sources at the Centriod location of Harvard CMT (N3.09^o, E94.50^o, depth=38.6 km). The two sources have same strike (320°) as well as the product of the dip angle and the seismic moment. The solid lines are calculated using the source with a seismic moment of 4x10^{22} Nm and a dip angle of 12°. The dashed lines are results of the source with seismic moment of 4x10^{22} Nm and a dip angle of 12°. They were slightly shifted downward. The top portion shows the comparison of the Rayleigh wave in vertical component and bottom shows the comparison of the transverse response (Love wave).

We also find that a joint analysis of Rayleigh and Love waves improves the resolution along the downdip direction of the slip distribution of a great subduction earthquake, in a finite fault study. Figure 3 compares synthetic long period responses at a representative station OBN for centroid at 5 km (black lines) and 20 km (red lines), respectively. We

used the moment tensor solution of the 2006 Kuril island earthquake (dip=15°; strike=220°) and bandpass filtered the synthetic seismograms from 3 to 6 mHz. Note that the peak amplitude of long period Rayleigh wave excited by the shallower source is 29% larger than that of the deeper one. In contrast, long period Love waves of two sources are indistinguishable. Then in this case, we are then able to determine the seismic moment using Love waves and proceed to resolve the depth of rupture using Rayleigh waves.

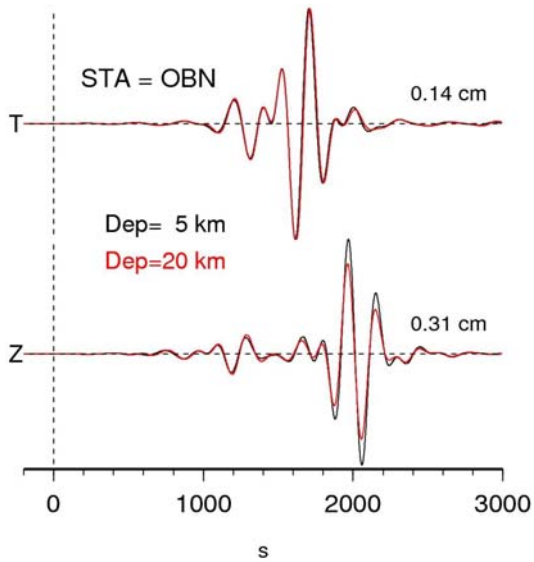

Figure 2. Comparison of synthetic vertical (Z) and Transverse (T) components at station OBN (Epicenter distance is 65° and azimuth is 326°). The red lines are results using a focal depth of 20 km and the black lines are results for focal depth of 5 km.

We have spent significant time to speed up the joint inversion. Using a lookup table approach, we are now able to reduce the computational time of the long period earth response for all subfault-station pairs (about 10,000 for the study of a typical earthquake) from hours to a few minutes.

We have also improved the performance of the data processing. The current system used the data flow of NEIC EDGE system. Several scripts were written to convert the IRIS SEED format to EDGE format, providing additional flexibility. For each earthquake, we convert all observations within teleseismic distances into displacements by removing the instrument responses, but then only select about 20 of them according to their signal-noise-ratios, azimuths, and epicenter distances. In an optimal condition, the entire processing could be accomplished in a few minutes, which makes it possible to obtain the preliminary inversion within a half-hour.

We have tested the joint inverse method extensively using previous earthquakes. Under the support of NEHRP proposal, *Shao and Ji* [2006] studied seven great (M>8) subduction earthquakes since 1990. *Ji and Shao* [2006] revisited four Tsunami earthquakes. Figure 3 shows an example, slip distribution of the 2006 Kuril island earthquake, the largest earthquake in year 2006. The result has been posted on NEIC webpage.

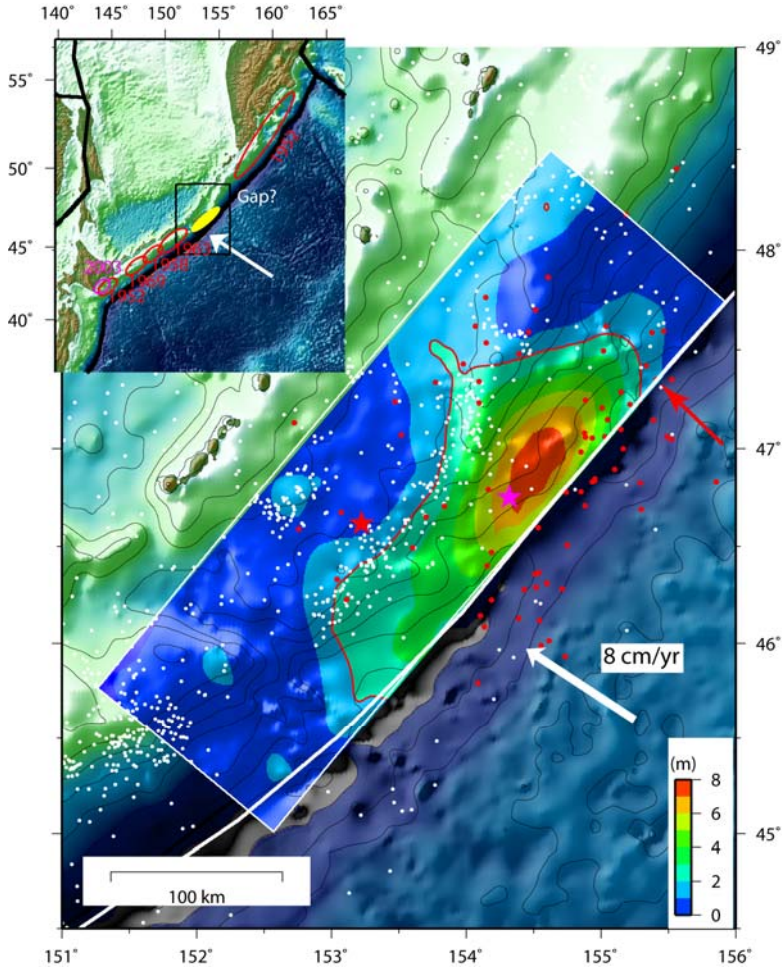

Figure 3. 2006 Kurile Islands earthquake. The yellow region in the insert map shows the rupture plane along with nearby major plane boundaries [*Bird*, 2003]. Red and pink ellipses indicate the rupture planes of six great subduction earthquakes (Mw>8) since 1950. Surface projection of a representative slip distribution (Model A) with intensity of the ETOP2 bathymetry map is shown in the main figure, against the relocated ISC seismicity (white dots), aftershock distribution (red dots), and the centroid location of Global CMT (pink star). The thin lines show the water depth in 1 km interval and the red line denotes the region with dislocation amplitudes larger than 2 m, 25% of peak slip. The white arrow shows the related plane motion between the Pacific plate and Okhotsk plate [NOVEL-1A, *Demets, et al.*, 1994].

Conclusions

We have developed and implemented the quick finite fault rupture inverse method using a joint teleseismic body and surface waveform inversion. Our recent results indicated that

- Additional long period surface waves help resolving the long-standing inconsistence between inversions based only on body waves and those based on

long period surface waves in terms of total scalar moments [e.g., *Beck and Ruff*, 1987; *Ekstrom*, 1989].

- Teleseismic body waves are capable of resolving the moment rate functions of large subduction earthquakes but lack of down-dip resolution for large subduction earthquakes sometimes. Additional surface waves are sensitive to the centroid depth, and improve the rupture distribution to the down-dip extension.

References

Beck, S. L., and L. J. Ruff (1987), Rupture Process Of The Great 1963 Kurile Islands Earthquake Sequence - Asperity Interaction And Multiple Event Rupture, *Journal Of Geophysical Research-Solid Earth And Planets*, *92*, 14123-14138.

Bird, P. (2003), An updated digital model of plate boundaries, *Geochemistry Geophysics Geosystems*, *4*.

Demets, C., et al. (1994), Effect Of Recent Revisions To The Geomagnetic Reversal Time-Scale On Estimates Of Current Plate Motions, *Geophys. Res. Lett.*, *21*, 2191-2194.

Ekstrom, G. (1989), A Very Broad-Band Inversion Method For The Recovery Of Earthquake Source Parameters, *Tectonophysics*, *166*, 73-100.

Kanamori, H., and J. W. Given (1981), Use of long-period surface waves for rapid determination of earthquake-source parameters, *Phys. Earth Planet. Inter.*, *27*, 8-31.

Kikuchi, M., and Y. Fukao (1987), Inversion Of Long-Period P-Waves From Great Earthquakes Along Subduction Zones, *Tectonophysics*, *144*, 231-247.

Kikuchi, M., and H. Kanamori (1991), Inversion of Complex Body Waves.3, *Bull. Seismol. Soc. Amer.*, *81*, 2335-2350.

Shao, G., and C. Ji (2006), Slip histories of six large subduction earthquakes from 1990 to 2004, *EOS Trans. AGU, 87 (52)*, Fall Meeting Suppl., Abstract S31A-0170.